Nonadiabatic interaction effects on population transfer in H_2 by stimulated Raman transition with partially overlapping laser pulses

Swaralipi Ghosh, Sanjay Sen, S. S. Bhattacharyya, and Samir Saha

Atomic and Molecular Physics Section, Department of Materials Science, Indian Association for the Cultivation of Science, Jadavpur, Calcutta 700032, India

We have theoretically investigated the population transfer in a four-level H_2 system by stimulated Raman transition from the ground $X\,^1\Sigma_g^+(\nu_g=0, J_g=0)$ level to higher rovibrational levels (ν_f, J_f) of the $X\,^1\Sigma_g^+$ state via the excited intermediate $B\,^1\Sigma_u^+(\nu_i=14, J_i=1)$ and $C\,^1\Pi_u^+(\nu_i=3, J_i=1)$ levels coupled with each other by nonadiabatic interaction, using time-dependent overlapping pump and Stokes laser fields. The density-matrix treatment, which permits the convenient inclusion of the spontaneous emissions from the intermediate levels, has been employed to describe the dynamics of the two-photon Raman resonance process. The present study performs the calculations of final populations (after both the pulses are over) of the ground and terminal levels for Q-branch $(J_f=0)$ fundamental $(\nu_f=1)$ and first overtone $(\nu_f=2)$ transitions and the S-branch $(J_f=2)$ fundamental $(\nu_f=1)$ transition as a function of time delay between the two pulses for the cases of on-resonance as well as off-resonance excitations in a wide range $(2\times10^5 - 2\times10^7 \text{ W/cm}^2)$ of peak intensities I_P^0 (I_S^0) of the pump (Stokes) fields. Both fields are assumed to have the same temporal shape, duration, peak intensities, and linear parallel polarizations. The accurate values of spontaneous radiative relaxation rates of the intermediate levels to the initial and final levels, taking into account their J and M dependence, are explicitly included in our calculations. The pulse width (full width at half maximum) τ_p is taken as 170 ns so that total spontaneous decay can occur during the pulse duration. The transfer efficiency is found to be very sensitive to the peak intensities of the laser pulses in each case of transition considered. Special attention is paid to the effects of the nonadiabatic (NA) interaction between $B(14,1)$ and $C(3,1)$ levels on population transfer efficiency. Calculations are also done in some particular cases using the adiabatic Born-Oppenheimer (ABO) approximation. The results with ABO approximation are found to differ remarkably from those obtained including NA interaction. Our calculations for the four-level H_2 system reveal that almost complete population is transferred in counterintuitive pulse order for both on-resonance and off-resonance excitations with intermediate and high values of I_P^0 (I_S^0). For intuitive pulse sequence also a large population transfer is achieved for on-resonance excitation at intermediate values of I_P^0 (I_S^0) and for off-resonance excitation at intermediate and high values of I_P^0 (I_S^0). [S1050-2947(99)02205-2]

PACS number(s): 42.50.Hz, 33.80.Be, 42.65.Dr

I. INTRODUCTION

The problem of selective and efficient population transfer to excited atomic or molecular levels not accessible by one-photon transition is of great interest in many applications, e.g., collision dynamics, spectroscopy, and optical control of chemical reactions. One of the most reliable techniques for selective excitation is the process of stimulated Raman adiabatic passage (STIRAP), which has been intensively studied numerically [1], analytically [2], and experimentally [3] in recent years. In its realization in a three-level Λ system, STIRAP requires three conditions: (i) two-photon resonance between the initially populated level and the final (terminal) level, (ii) counterintuitive pulse order in which the Stokes pulse, driving the transition between the intermediate and final levels, precedes the pump pulse, though they must overlap partially, and (iii) adiabatic time evolution.

Band and Julienne [1] were the first to report the numerical results of calculations for Na_2 molecules describing the dynamics of the STIRAP process using a full density-matrix method. The results compared well with the experimentally measured values [3] for on-resonance and off-resonance excitations. Recently, Vitanov and Stenholm [2] have carried

out a detailed analytical investigation of this STIRAP process in three-level model systems. They have presented an analytically solvable model for this process with intermediate level resonance. Various features of population transfer by delayed pulses in this model were deduced analytically with particular emphasis on the effect of the pulse order on transfer efficiency. They have also analyzed the effect of intermediate level detuning as well as irreversible dissipation from the intermediate level on the efficiency of the STIRAP process. The effect of dissipation was found to be more pronounced for the intuitive pulse sequence as the intermediate level becomes significantly populated during the transfer. The spontaneous decay of the intermediate level to the initial or final level was not considered. Stenholm and co-workers have also examined analytically and numerically the role of incoherent ionization channels, Stark shifts, and the nonzero Fano parameter on the efficiency of population transfer between two discrete states via a common continuum [4]. Bergmann and his co-workers [3] first demonstrated experimentally and analyzed the novel concept of STIRAP for efficient population transfer of vibrational levels in Na_2 molecules. In spite of the fact that the excited state has a decay time shorter than the laser pulse duration, almost complete

population transfer occurred for counterintuitive sequence of pulses when the pump and Stokes frequencies were tuned to resonance. These experimental findings were described in terms of the adiabatic passage, wherein an electric-field-dressed eigenstate evolves from the ground molecular state to the final state as a time-dependent linear combination of the ground and final states with zero amplitude of the intermediate excited state. However, this adiabatic passage description treats the system within the context of an adiabatic Hamiltonian approximation without the explicit inclusion of the spontaneous decay rate of the intermediate state. Inclusion of the spontaneous decay back to the initial or final level cannot be properly carried out within a wave-function picture. A density-matrix description is appropriate in which decay mechanisms can be explicitly incorporated by introducing decay terms into the Liouville equation (sometimes called the Bloch equation).

In the present paper, we have investigated the population transfer in a four-level system in H_2 molecule in the presence of pump and Stokes laser fields. To our knowledge, this is the first work where such calculations are done for a real four-level system in which the two very close intermediate levels are strongly coupled with each other by nonadiabatic interaction. The full density-matrix formalism has been adopted for this study. It is a well-known method for treating the dynamics of multilevel systems interacting with external time-dependent fields in the presence of all possible relaxations. The decay rates of the intermediate levels due to the spontaneous radiative emission to the initial and final levels along with the relaxation out of the four-level system have been incorporated explicitly. Specifically, the calculation of population transfer has been performed from the ground $X\,^1\Sigma_g^+(\nu_g=0, J_g=0)$ level to the final $X\,^1\Sigma_g^+(\nu_f, J_f)$ level via the intermediate $B\,^1\Sigma_u^+(\nu_i=14, J_i=1)$ and $C\,^1\Pi_u^+(\nu_i=3, J_i=1)$ levels of H_2. We have studied in detail the dependence of the population transfer on the time delay between the pump and Stokes pulses for the cases of on-resonance and off-resonance excitations in a wide range of peak intensities $(2\times10^5 - 2\times10^7\ \mathrm{W/cm}^2)$ of the pump (Stokes) fields. The two fields are considered to have the same peak intensity, pulse shape, duration, and linear parallel polarizations.

The present paper reveals interesting features of the influence of the nonadiabatic (NA) interaction between the two bare, nearly degenerate intermediate levels on the transfer efficiency. This electronic-rotational coupling between the intermediate $B(14,1)$ and $C(3,1)$ levels due to intramolecular configuration interaction [5] is seen to play a very important role in determining the population transfer in H_2. To assess the effects of NA interaction on the population transfer, calculations are also done for some special cases using the adiabatic Born-Oppenheimer (ABO) approximation. It should be stressed here that the nonadiabatic interaction [5] considered in this paper is not to be confused with the ''nonadiabatic coupling'' used [1(c),3(b)] in the context of STIRAP. Our nonadiabatic interaction arises due to the effect of molecular nuclear motion on neighboring Born-Oppenheimer electronic states even in the absence of radiative coupling and is very significant for light molecules like H_2 [6].

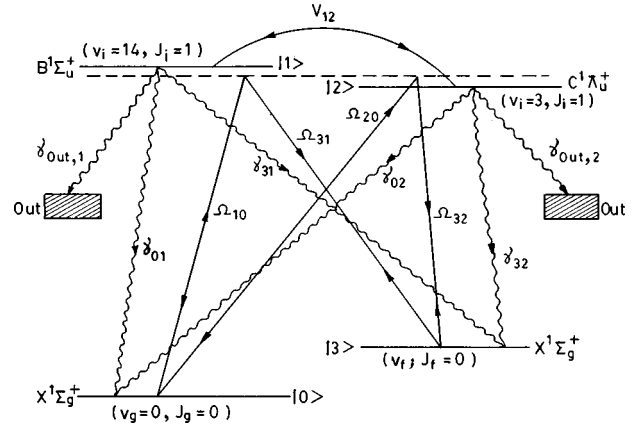The remaining part of the paper is organized as follows.

FIG. 1. Schematic diagram of the four-level H_2 system interacting with the pump and Stokes lasers where all state labels, the relevant Rabi frequencies, as well as the spontaneous decay rates are indicated. Ω_{ji} denotes the time-dependent one-photon coupling matrix element for Rabi transition from level $|i\rangle$ to level $|j\rangle$ by the pump or Stokes field. V_{12} is the nonadiabatic interaction matrix element between $|1\rangle$ and $|2\rangle$. γ_{01} (γ_{02}) and γ_{31} (γ_{32}) denote the spontaneous radiative decay rates from level $|1\rangle$ ($|2\rangle$) to levels $|0\rangle$ and $|3\rangle$. $\gamma_{\mathrm{out},1}$ ($\gamma_{\mathrm{out},2}$) denotes the decay rates of level $|1\rangle$ ($|2\rangle$) to other levels out of the four-level system considered.

Section II develops the necessary density-matrix formalism for the four-level system with the NA interaction to evaluate the population transfer. In Sec. III, the way the calculation has been done is presented. Section IV discusses the numerical results of various transitions for different values of detuning and intensities of the laser fields. The paper ends with a brief conclusion in Sec. V.

II. FORMULATION

This section describes the density-matrix formulation of population transfer in H_2 using time-dependent overlapping pump and Stokes laser fields by stimulated Raman transition from the ground $X\,^1\Sigma_g^+(\nu_g=0, J_g=0)$ level to higher rovibrational levels (ν_f, J_f) of $X\,^1\Sigma_g^+$ state. The nearly degenerate excited intermediate levels $B\,^1\Sigma_u^+(\nu_i=14, J_i=1)$ and $C\,^1\Pi_u^+(\nu_i=3, J_i=1)$ are strongly coupled to each other through nonadiabatic electronic-rotational interaction. The four-level system under consideration is shown schematically in Fig. 1 where all state labels, the relevant Rabi frequencies, as well as the spontaneous decay rates are indicated. Here $|0\rangle$ and $|3\rangle$ specify the ground and final (terminal) levels, respectively. Among the two intermediate levels, $B\,^1\Sigma_u^+(\nu_i=14, J_i=1)$ is denoted by $|1\rangle$ while $C\,^1\Pi_u^+(\nu_i=3, J_i=1)$ as $|2\rangle$. Level $|0\rangle$ is coupled with two intermediate levels $|1\rangle$ and $|2\rangle$ by the pump field whereas the Stokes field drives the transitions from $|1\rangle$ and $|2\rangle$ to final level $|3\rangle$. $|0\rangle$ and $|3\rangle$ being the levels of same parity, the transition between them is electric dipole forbidden. It may be noted here that the intermediate level $C\,^1\Pi_u^-(\nu_i=3, J_i=1)$ is not optically accessible from the ground $X\,^1\Sigma_g^+(\nu_g=0, J_g=0)$ level. As we have taken $J_g=0$ (hence $M_g=0$) and linear parallel polarizations of the laser fields, the Rabi transitions involving $M_i=0$ only (since $\Delta M=0$) will be allowed and the other optical transitions with $M_i=\pm1$ (since $J_i=1$) will vanish. Hence, the H_2 system considered by us

reduces to a four-level system.

The Liouville equation for the density-matrix operator $(\rho(t))$ of the four-level system interacting with two time-dependent laser fields including phenomenologically decay (Γ) due to spontaneous emission, is given by (in a.u.)

$$\frac{d\rho(t)}{dt} = -i[H,\rho] - \Gamma\rho, \qquad (1)$$

where $H(t) = H_O + H_I(t) + H_{NA}$ is the total time-dependent Hamiltonian of the system. H_O is the Hamiltonian of the unperturbed molecule. $H_I(t)$ denotes the interaction Hamiltonian between the molecule and the fields, which in the electric-field or length-gauge form (with dipole approximation) can be expressed as

$$H_I(t) = -\vec{E}_P(t)\cdot\vec{d} - \vec{E}_S(t)\cdot\vec{d}. \qquad (2)$$

$\vec{d}$ denotes the transition dipole operator whereas $\vec{E}_P(t)$ and $\vec{E}_S(t)$ are the time-dependent electric field vectors of the pump and Stokes lasers, respectively. The classical forms of $\vec{E}_P(t)$ and $\vec{E}_S(t)$ for linearly polarized light, are given by

$$\vec{E}_P(t) = \tfrac{1}{2} f_P(t) F_P^0 \hat{\varepsilon}_P [e^{i\omega_P t} + e^{-i\omega_P t}] \qquad (3a)$$

and

$$\vec{E}_S(t) = \tfrac{1}{2} f_S(t) F_S^0 \hat{\varepsilon}_S [e^{i\omega_S t} + e^{-i\omega_S t}], \qquad (3b)$$

where ω_P and ω_S are the frequencies of the assumed single-mode fields, $\hat{\varepsilon}_P$ and $\hat{\varepsilon}_S$ represent the unit polarization vectors of the incident linearly polarized pump and Stokes fields, while $f_P(t)$ and $f_S(t)$ express the time variation of the field amplitudes of peak values F_P^0 and F_S^0, respectively. The functional forms of $f_P(t)$ and $f_S(t)$ are taken to be Gaussian [1],

$$f_P(t) = \exp[-(t-t_p)^2/2\tau_p^2], \qquad (4a)$$

and

$$f_S(t) = \exp[-\{t-(t_p+\Delta t)\}^2/2\tau_p^2], \qquad (4b)$$

with full width [full width at half maximum (FWHM)] τ_p and time delay between the pulses Δt. t_p is the pulse scaling time. $\Delta t > 0$ specifies the intuitive pulse order in which the pump pulse preceeds the Stokes pulse, whereas $\Delta t < 0$ corresponds to the counterintuitive sequence of interaction, which begins with the Stokes pulse and ends with the pump pulse. H_{NA} is the nonadiabatic interaction Hamiltonian due to electronic-rotational coupling between intermediate levels $|1\rangle$ and $|2\rangle$. Its matrix element is given by [5]

$$V_{12} = \langle 1|H_{NA}|2\rangle = \langle 2|H_{NA}|1\rangle$$

$$= -\frac{\sqrt{J_i(J_i+1)}}{2\mu}\langle 1|\{S(R)/R^2\}|2\rangle, \qquad (5a)$$

where $S(R) = 2^{1/2}\langle\Psi_B(\Lambda=0)|L^+|\Psi_C(\Lambda=-1)\rangle$

$$= 2^{1/2}\langle\Psi_B(\Lambda=0)|L^-|\Psi_C(\Lambda=+1)\rangle. \qquad (5b)$$

Using the Liouville equation (1), the optical Bloch equations for the elements of density-matrix operator $\rho(t)$ governing the time evolution of the four-level system, within the rotating wave approximation, can be written as

$$\frac{d\sigma_{00}(t)}{dt} = -i(\Omega_{01}\sigma_{10}-\Omega_{10}\sigma_{01}) - i(\Omega_{02}\sigma_{20}-\Omega_{20}\sigma_{02})$$
$$+ \gamma_{01}\sigma_{11} + \gamma_{02}\sigma_{22}, \qquad (6a)$$

$$\frac{d\sigma_{11}(t)}{dt} = -i(\Omega_{10}\sigma_{01}-\Omega_{01}\sigma_{10}) - i(V_{12}\sigma_{21}-V_{21}\sigma_{12})$$
$$- i(\Omega_{13}\sigma_{31}-\Omega_{31}\sigma_{13}) - \Gamma_1\sigma_{11}, \qquad (6b)$$

$$\frac{d\sigma_{22}(t)}{dt} = -i(\Omega_{20}\sigma_{02}-\Omega_{02}\sigma_{20}) - i(V_{21}\sigma_{12}-V_{12}\sigma_{21})$$
$$- i(\Omega_{23}\sigma_{32}-\Omega_{32}\sigma_{23}) - \Gamma_2\sigma_{22}, \qquad (6c)$$

$$\frac{d\sigma_{33}(t)}{dt} = -i(\Omega_{31}\sigma_{13}-\Omega_{13}\sigma_{31}) - i(\Omega_{32}\sigma_{23}-\Omega_{23}\sigma_{32})$$
$$+ \gamma_{31}\sigma_{11} + \gamma_{32}\sigma_{22}, \qquad (6d)$$

$$\frac{d\sigma_{10}(t)}{dt} = i\Omega_{10}(\sigma_{11}-\sigma_{00}) - i(V_{12}\sigma_{20}-\Omega_{20}\sigma_{12}) - i\Omega_{13}\sigma_{30}$$
$$+ \left(i\Delta_1 - \frac{\Gamma_1}{2}\right)\sigma_{10}, \qquad (6e)$$

$$\frac{d\sigma_{20}(t)}{dt} = i\Omega_{20}(\sigma_{22}-\sigma_{00}) - i(V_{21}\sigma_{10}-\Omega_{10}\sigma_{21}) - i\Omega_{23}\sigma_{30}$$
$$+ \left(i\Delta_2 - \frac{\Gamma_2}{2}\right)\sigma_{20}, \qquad (6f)$$

$$\frac{d\sigma_{30}(t)}{dt} = -i(\Omega_{31}\sigma_{10}-\Omega_{10}\sigma_{31}) - i(\Omega_{32}\sigma_{20}-\Omega_{20}\sigma_{32})$$
$$+ i\Delta\sigma_{30}, \qquad (6g)$$

$$\frac{d\sigma_{21}(t)}{dt} = -i(\Omega_{20}\sigma_{01}-\Omega_{01}\sigma_{20}) - iV_{21}(\sigma_{11}-\sigma_{22})$$
$$+ [i(\omega_1-\omega_2) - \tfrac{1}{2}(\Gamma_2+\Gamma_1)]\sigma_{21} - i(\Omega_{23}\sigma_{31}$$
$$- \Omega_{31}\sigma_{23}), \qquad (6h)$$

$$\frac{d\sigma_{31}(t)}{dt} = i\Omega_{31}(\sigma_{33}-\sigma_{11}) - i(\Omega_{32}\sigma_{21}-V_{21}\sigma_{32})$$
$$+ \left[i\{(\omega_1-\omega_3)-\omega_S\} - \frac{\Gamma_1}{2}\right]\sigma_{31} + i\Omega_{01}\sigma_{30}, \qquad (6i)$$

$$\frac{d\sigma_{32}(t)}{dt} = i\Omega_{32}(\sigma_{33}-\sigma_{22})-i(\Omega_{31}\sigma_{12}-V_{12}\sigma_{31})$$

$$+\left[i\{(\omega_2-\omega_3)-\omega_S\}-\frac{\Gamma_2}{2}\right]\sigma_{32}+i\Omega_{02}\sigma_{30}.$$

(6j)

The rest of the 16 equations are obtained by using the relation $\sigma_{ij}=\sigma_{ji}^*$. $\sigma(t)$ is the slowly varying matrix operator whose elements are related to those of $\rho(t)$ by the defining equations $\rho_{ii}(t)=\sigma_{ii}(t)$, $\rho_{10}(t)=\sigma_{10}(t)e^{-i\omega_p t}$, etc. Ω_{ji} denotes the time-dependent one-photon coupling matrix element for Rabi transition from the state $|i\rangle$ to the state $|j\rangle$ by the pump or Stokes field and is given by $-\frac{1}{2}f_{P,S}(t)F_{P,S}^0\langle j|(\hat{\varepsilon}_{P,S}\cdot\vec{d})|i\rangle$. It should be noted here that in Eqs. (6e) and (6f), Δ_1, Δ_2 are the detunings of the pump-laser frequency from the adiabatic energy difference between (unperturbed) levels $|1\rangle$, $|2\rangle$, and $|0\rangle$ and are given by $\Delta_1=\hbar\omega_p-(E_1-E_0)$, $\Delta_2=\hbar\omega_p-(E_2-E_0)$. E_0 is the energy of the ground level $|0\rangle$ while E_1^0 and E_2^0 are the adiabatic energies of levels $|1\rangle$ and $|2\rangle$. The expression for Δ is given by $\Delta=(\omega_p-\omega_s)-(E_3-E_0)$ where E_3 is the energy of the final level $|3\rangle$. For two-photon Raman resonance Δ, in Eq. (6g), is 0. In Eqs. (6), the diagonal matrix elements $\sigma_{00}(t)$, $\sigma_{11}(t)$, $\sigma_{22}(t)$, and $\sigma_{33}(t)$ denote the populations of the corresponding levels whereas the off-diagonal elements $\sigma_{10}(t)$, $\sigma_{20}(t)$, etc., are interpreted as the coherences. Γ_1 and Γ_2 represent the total radiative decay rates of levels $|1\rangle$ and $|2\rangle$, respectively. The terms Γ_1 and Γ_2 introduce a coherence loss in the transfer process. Along with the spontaneous decay to the ground and final levels, the levels $|1\rangle$ and $|2\rangle$ can decay to other levels out of this four-level system. The spontaneous emissions from level $|1\rangle$ ($|2\rangle$) to levels $|0\rangle$ and $|3\rangle$ are explicitly represented by the decay rates γ_{01} (γ_{02}) and γ_{31} (γ_{32}). The relaxations ($\gamma_{out,1}$ and $\gamma_{out,2}$) to other levels out of the four-level system considered here are taken into account in Γ_1 ($=\gamma_{01}+\gamma_{31}+\gamma_{out,1}$) and Γ_2 ($=\gamma_{02}+\gamma_{32}+\gamma_{out,2}$). We have neglected photodissociation/photoionization of the molecule from the intermediate states. This is justified at the level of fluences that we have considered. The two-photon dissociation/ionization channel out of the ground state will not contribute either. Since we are concerned here only with the on-resonance or near-resonance excitations and the intensities of the two pulsed fields are not too high, the ac Stark shifts of levels $|1\rangle$, $|2\rangle$, and $|0\rangle$ have not been taken into consideration. We have also neglected the collisional relaxations of the level $|1\rangle$, $|2\rangle$, and $|3\rangle$ since they are negligible in a beam experiment [3].

The set of Eqs. (6) can be written in a matrix form as

$$\dot{\sigma}=M\sigma.$$

(7)

It may be noted that here M is a non-Hermitian and asymmetric matrix though $\Omega_{ij}=\Omega_{ij}^*$ and $V_{12}=V_{12}^*$.

Equation (7) can be solved in a similar way as discussed in our earlier paper [7]. The evaluated diagonal elements $\sigma_{ii}(t)$, $i=0-3$ describe the populations at time t of the four-level system interacting with the two laser fields in counterintuitive or intuitive pulse order. Thus the final populations

of the levels, viz., $P_g=\sigma_{00}(\infty)$, $P_f=\sigma_{33}(\infty)$, etc., after the pulses are over can be evaluated.

III. CALCULATIONS

We have calculated the final populations (after the pump and Stokes pulses are over) of the ground and final levels of H_2 for Q-branch ($J_f=0$) fundamental ($\nu_f=1$) and first overtone ($\nu_f=2$) transitions as well as the S-branch ($J_f=2$) fundamental ($\nu_f=1$) transition from the ground $X\,^1\Sigma_g^+(\nu_g=0,J_g=0)$ level to the final $X\,^1\Sigma_g^+(\nu_f,J_f)$ level via the intermediate $B\,^1\Sigma_u^+(\nu_i=14,J_i=1)$ and $C\,^1\Pi_u^+(\nu_i=3,J_i=1)$ levels coupled by nonadiabatic interaction with each other [6]. We have investigated in detail the dependence of population transfer on the time displacement between the pump and Stokes pulses for the cases of on-resonance and off-resonance excitations in a wide range ($2\times10^5-2\times10^7$ W/cm^2) of peak intensities [$I_{P,S}^0=c(F_{P,S}^0)^2/8\pi$] of the pump (Stokes) fields. To assess the effects of NA interaction on the population transfer, the same calculations are also done using the ABO approximation [i.e., clamped nuclei or Born-Oppenheimer (BO) approximation with adiabatic correction] for some specific cases. The transition wavelengths of the pump laser for resonance to the perturbed B(14,1) and C(3,1) levels are about 94.6 nm. The two laser pulses are considered to have the same peak intensity, shape, duration, and linear parallel polarizations. The pulse width (FWHM) τ_p is taken as 170 ns so that total spontaneous radiative relaxation from the intermediate levels can occur during the pulse duration.

The BO potential energies and the adiabatic corrections to them for B, C, and X states are obtained from Wolniewicz and Dressler [8] and others [9]. Electronic transition dipole moments for $X-B(C)$ states are taken from Wolniewicz [10]. The potential and dipole moments are interpolated using the cubic spline interpolation method [11]. The radial bound wave functions are generated by solving numerically the radial Schrödinger equation with the well-known Numerov-Cooley method [12]. The Simpson integration rule is used to carry out the integrations for the single-photon matrix elements. The nonadiabatic energies of $B(14,1)$ and $C(3,1)$ are given by Senn, Quadrelli, and Dressler [13]. The values of the spontaneous decay rates, $\gamma_{out,1}$ and $\gamma_{out,2}$, are obtained from Dalgarno and co-workers [14]. The radiative spontaneous emission from any discrete rovibrational level couples different possible rotational levels and their magnetic sublevels and each of them contributes differently in determining the values of the decay rates. We have incorporated J and M dependence properly in the values of γ_{01}, γ_{31}, Γ_1, etc. The values of Ω_{ji}, γ_{ij}, Γ_j, and V_{12} are given in Table I.

IV. RESULTS AND DISCUSSIONS

In Fig. 2, the populations of the ground and final levels designated as P_g and P_f, respectively, for the Q-branch ($J_f=0$) fundamental ($\nu_f=1$) transition from the initial $X\,^1\Sigma_g^+(\nu_g=0,J_g=0)$ level of H_2 molecule are shown as a function of the reduced time delay ($D=\Delta t/\tau_P$) for on-resonance excitation to the nonadiabatically perturbed $B\,^1\Sigma_u^+(\nu_i=14,J_i=1)$ level ($\Delta_1=1.79$ cm^{-1}). The profiles

TABLE I. Values (in cm^{-1}) of Rabi frequencies (Ω_{ji}), state-to-state spontaneous decay rates (γ_{ij}), and total spontaneous decay rates (Γ_j) for different transitions. The nonadiabatic interaction matrix element between the levels $|1\rangle$ and $|2\rangle$ is $V_{12} = -13.06\,cm^{-1}$. I_P (I_S) is in W/cm^2.

| | Q-branch ($J_f=0$) | | S-branch ($J_f=2$) |
	fundamental ($v_f=1$)	first overtone ($v_f=2$)	fundamental ($v_f=1$)
Ω_{10}	$-6.15(-5)^a \sqrt{I_P}$	$-6.15(-5) \sqrt{I_P}$	$-6.15(-5) \sqrt{I_P}$
Ω_{20}	$1.39(-4) \sqrt{I_P}$	$1.39(-4) \sqrt{I_P}$	$1.39(-4) \sqrt{I_P}$
Ω_{31}	$5.26(-5) \sqrt{I_S}$	$1.89(-5) \sqrt{I_S}$	$4.88(-5) \sqrt{I_S}$
Ω_{32}	$-2.87(-5) \sqrt{I_S}$	$-1.27(-4) \sqrt{I_S}$	$1.55(-5) \sqrt{I_S}$
γ_{01}	$1.32(-3)$	$1.32(-3)$	$1.32(-3)$
γ_{02}	$6.80(-3)$	$6.80(-3)$	$6.80(-3)$
γ_{31}	$8.58(-4)$	$9.84(-5)$	$7.32(-4)$
γ_{32}	$2.55(-4)$	$4.47(-3)$	$7.36(-5)$
Γ_1	$2.78(-2)$	$2.87(-2)$	$2.76(-2)$
Γ_2	$3.73(-2)$	$3.74(-2)$	$3.71(-2)$

$^a-6.15(-5) = -6.15 \times 10^{-5}$.

are studied for different values of peak intensities I_P^0 and I_S^0 of pump and Stokes laser fields having linear parallel polarizations and pulse width (FWHM) τ_p as 170 ns.

Figure 2(a) exhibits the variation of the P_g and P_f against D for low intensities I_P^0 (I_S^0) = 2×10^5 W/cm^2. The final level population is observed to possess two maxima, one for the counterintuitive pulse order ($D<0$) and another for the intuitive pulse order ($D>0$). The P_f profile is almost symmetric about $D=0$, though the optimal population transfer is only ~63% around $D = \mp 1.5$. P_f becomes almost zero for $D \leq -4$ or $D \geq +4$ as the overlap of the intensity profiles of the two lasers is very small there and population remains totally in the ground level.

Figures 2(b) and 2(c) present the P_g and P_f profiles with D for intermediate intensities I_P^0 (I_S^0) = 1×10^6 W/cm^2 and 2×10^6 W/cm^2, respectively. With the increase of intensities from low to intermediate values, the maximum value of P_f is enhanced enormously but the profiles begin to show asymmetry about $D=0$, which is more prominent for I_P^0 (I_S^0) = 2×10^6 W/cm^2. For I_P^0 (I_S^0) = 1×10^6 W/cm^2 [Fig. 2(b)], total transfer is achieved around $D=-2$ and about 92% population is transferred around $D=+2$. For I_P^0 (I_S^0) = 2×10^6 W/cm^2 [Fig. 2(c)], complete population is transferred to the final level when Stokes pulse precedes the pump pulse by $2\tau_p$ ($D=-2$) and the population transfer is about 84% around $D=+2$.

In Figs. 2(d) and 2(e), we present the profiles for I_P^0 (I_S^0) = 1×10^7 W/cm^2 and 2×10^7 W/cm^2, respectively. At these high values of I_P^0 (I_S^0), there is a dramatic change in the final-state population with almost complete destruction of the symmetric nature of the P_f profiles. Also as I_P^0 (I_S^0) is increased to higher value, transfer efficiency begins to fall for $D \geq 0$. At I_P^0 (I_S^0) = 1×10^7 W/cm^2 [Fig. 2(d)], total transfer occurs with a broad peak around $D=-2.5$ and the transfer efficiency is about 43% around $D=+2.5$ For I_P^0 (I_S^0) = 2×10^7 W/cm^2 [Fig. 2(e)], complete transfer is achieved with a broader peak around $D=-3$ and the transfer is only ~18%

around $D = +3$. At these high intensities the second peak is more like a shoulder than a peak.

It may be pointed out here that even with a 170-ns pulse, much longer than the spontaneous lifetimes, the spontaneous decay does not play a larger role in either the counterintuitive or intuitive region at low intensities I_P^0 (I_S^0) = 2×10^5 W/cm^2 [Fig. 2(a)], as shown by the fact that the final and ground-level populations add up to unity here, with negligible population losses. This may be explained as follows. For low intensities, Rabi frequencies are not large and the intermediate levels are never significantly populated throughout the pulse duration. This gives rise to negligible overall population loss, even for such a long pulse. But for intermediate and higher intensities I_P^0 (I_S^0) = 1×10^6 – 2×10^7 W/cm^2 [Figs. 2(b)–2(e)], there is appreciable population loss in the whole intuitive region ($D>0$) and in the counterintuitive region where the two pulses have negligible overlap in time, i.e., where $D \ll 0$. The sum of the final and ground-level populations does not become unity in these regions. This is a consequence of the fact that larger Rabi frequencies cause accumulation of some population in the intermediate levels at some point in time, which then decay by spontaneous emissions out of the (four-level) system during the pulse duration. This gives rise to significant population loss there. However, the populations of the excited intermediate levels remain virtually zero at the end of the pulses because the spontaneous decay times of these levels are shorter than the pulse duration.

For higher values of peak intensities, the P_f profiles extend to more negative and positive values of D. In the region of $D < -5$, whatever small transfer occurs, takes place only as a result of spontaneous emission of the intermediate levels to the final level. Also for $D > +5$, the molecules excited to the intermediate levels by pump pulse decay mainly to other levels than the final one by spontaneous emission before they experience the Stokes pulse yielding a very small population transfer into the final level.

It is interesting to note that as I_P^0 (I_S^0) increases from 2×10^5 W/cm^2 to 2×10^7 W/cm^2, the total transfer of population to the final level occurs at more and more negative values of D with a wider peak. In contrast to the results of the three-level system (viz., Na_2) studied earlier [1,3], we see that for our four-level system (H_2) with two intermediate coupled levels, large population transfer also takes place in intuitive pulse order ($D>0$) for on-resonance excitation and intermediate values of I_P^0 (I_S^0). This is an interesting feature. The underlying physics behind this may be explained as follows. The NA interaction between the two electronic states $B\,^1\Sigma_u^+$ and $C\,^1\Pi_u^+$ mixes the two close lying ABO levels $\nu=14$ and $J=1$ of B state and $\nu=3$ and $J=1$ of C state so that two new perturbed eigenstates with mixed Σ^+ and Π^+ characters are created. The perturbed B level is one of the mixed eigenstates, which has ~73% B character and ~27% C character while the perturbed C level is the other mixed eigenstate with ~73% C character and ~27% B character [13]. The respective energies of the perturbed B and C levels are $E_1 = -12687.87\,cm^{-1}$ and $E_2 = -12716.44\,cm^{-1}$ while our calculated adiabatic (ABO) energies of the unperturbed B and C levels are $E_1^0 = -12689.66\,cm^{-1}$ and $E_2^0 = -12706.88\,cm^{-1}$, respectively with respect to the ABO threshold of the B/C state. The population transfer due to the
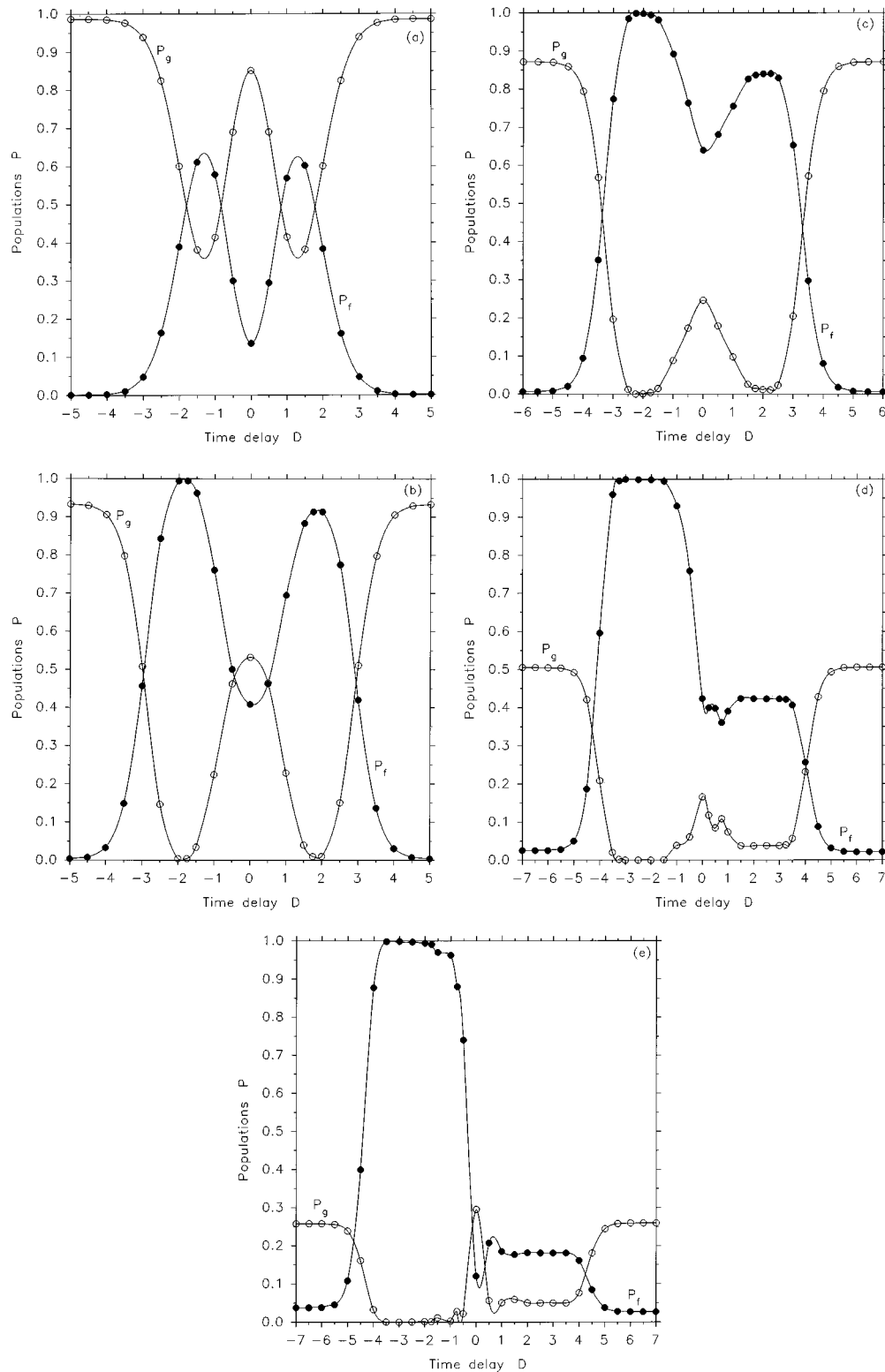
FIG. 2. Populations of the ground (P_g) and final (P_f) levels (after the pump and Stokes laser pulses are over) plotted against (reduced) time delay ($D = \Delta t / \tau_p$) between the pulses for the Q-branch ($J_f = 0$) fundamental ($\nu_f = 1$) transition from $X(\nu_g = 0, J_g = 0)$ level for resonance with the intermediate perturbed $B(14,1)$ level for $\tau_p = 170$ ns and different values of I_P^0 (I_S^0) including the NA interaction (V_{12}) between $B(14,1)$ and $C(3,1)$ levels. (a) I_P^0 (I_S^0) $= 2 \times 10^5$ W/cm^2, (b) I_P^0 (I_S^0) $= 1 \times 10^6$ W/cm^2, (c) I_P^0 (I_S^0) $= 2 \times 10^6$ W/cm^2, (d) I_P^0 (I_S^0) $= 1 \times 10^7$ W/cm^2, and (e) I_P^0 (I_S^0) $= 2 \times 10^7$ W/cm^2.

on-resonance excitation to the perturbed B level may, therefore, be viewed to result from a mixture of off-resonance excitations to the unperturbed ABO B level with ~73% B character and unperturbed ABO C level with ~27% C char-

acter. Thus, as in the case of off-resonance excitation for the three-level system like Na$_2$ or our four-level unperturbed ABO H$_2$ system as discussed later in this section, we get a large or significant population transfer for intuitive pulse or-
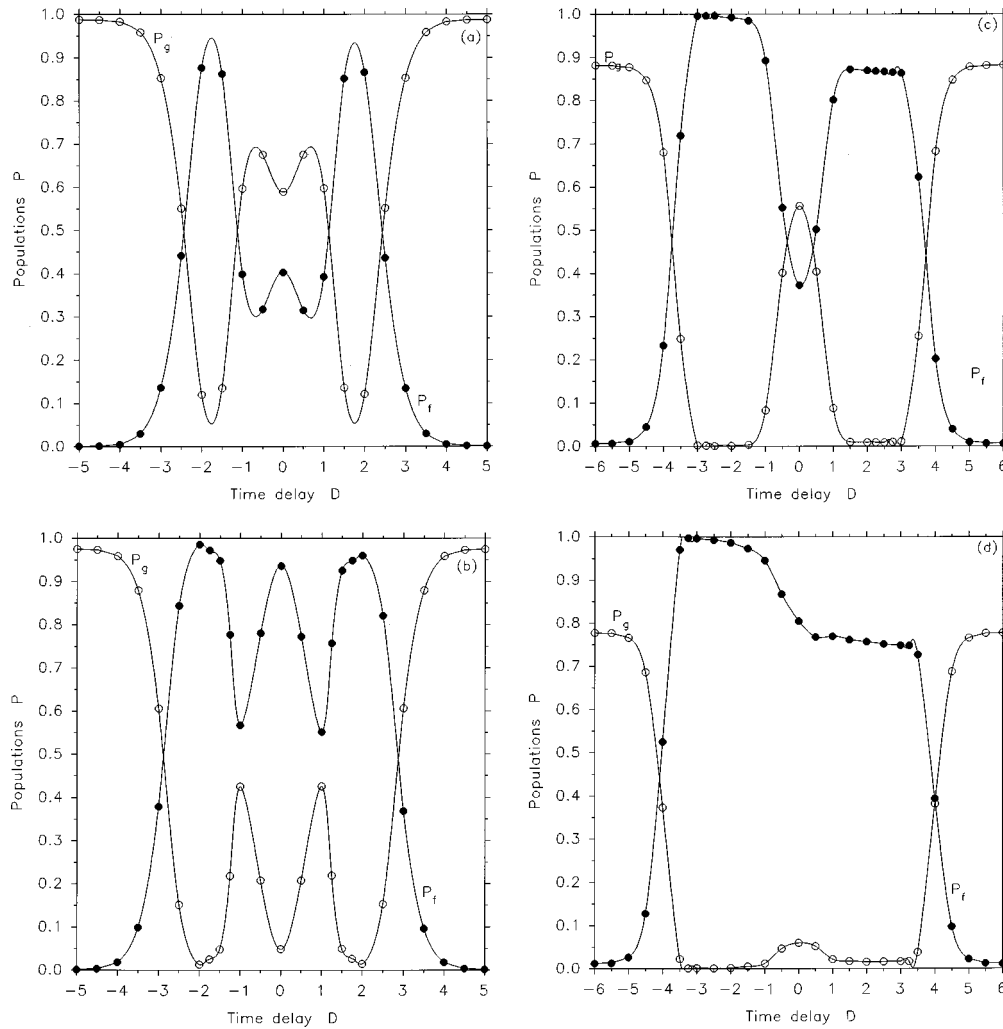
FIG. 3. Same as Fig. 2 except for the frequency of the pump laser detuned by -10.40 cm^{-1} with respect to the nonadiabatically perturbed $B(14,1)$ level. (a) I_P^0 (I_S^0) $=1\times10^6$ W/cm^2, (b) I_P^0 (I_S^0) $=2\times10^6$ W/cm^2, (c) I_P^0 (I_S^0) $=1\times10^7$ W/cm^2, and (d) I_P^0 (I_S^0) $=2\times10^7$ W/cm^2.

der also for on-resonance excitation to the perturbed B level. Like the three-level system, total transfer is achieved in counterintuitive pulse sequence ($D<0$) for on-resonance excitation with intermediate as well as high values of I_P^0 (I_S^0) in our four-level system. The interpretation of this follows from the formulations of STIRAP given in [1–3].

In Fig. 3, P_g and P_f profiles are shown for the pump laser detuned by -10.40 cm^{-1} ($\Delta_1=-8.61$ cm^{-1}), with respect to the nonadiabatically perturbed $B(14,1)$ level, corresponding to the situation when the pump laser reaches midway the unperturbed ABO $B(14,1)$ and $C(3,1)$ levels. Here also the population versus delay profiles are found to be very sensitive to the change of intensities.

At intermediate peak intensities of 1×10^6 W/cm^2 [Fig. 3(a)] or 2×10^6 W/cm^2 [Fig. 3(b)], the P_f profiles are nearly symmetrical about $D=0$. At I_P^0 (I_S^0) $=1\times10^6$ W/cm^2, maximum 95% population transfer is obtained around $D=\mp2$. But at I_P^0 (I_S^0) $=2\times10^6$ W/cm^2, the final level population is increased to a maximum value of about 99% around $D=\mp2$. In Fig. 3(b), an interesting feature is the appearance of a prominent third peak in the P_f curve at zero time displacement ($D=0$). Though the P_f value at this third peak is somewhat smaller than those at the major peaks at $D\simeq\pm2$, still it is much larger than the P_f values at $D=\pm1$. About

95% population transfer occurs for this case of two completely overlapping pulses ($D=0$). This may also be interpreted within the framework of the standard STIRAP theory.

Further increase of I_P^0 (I_S^0) to high values of 1×10^7 W/cm^2 [Fig. 3(c)] or 2×10^7 W/cm^2 [Fig. 3(d)] leads to destruction of the symmetry in the profiles and the transfer probability is reduced to some extent at $D>0$. At I_P^0 (I_S^0) $=1\times10^7$ W/cm^2, total transfer occurs with a broad peak around $D=-2.5$ while the transfer is about 87% around $D=+2.5$, again with a wide peak. At I_P^0 (I_S^0) $=2\times10^7$ W/cm^2, complete transfer is obtained around $D=-2.5$ and $\sim$76% transfer occurs around $D=+1.5$ with a shoulder rather than a peak. It is to be mentioned here that for the high intensities considered, the population transfer at $D>0$ is larger relative to the corresponding values for on-resonance excitation. The reason may be the loss mechanisms due to the decay terms, which are less effective for off-resonance excitation.

The final population profiles corresponding to the Q-branch ($J_f=0$) first overtone ($\nu_f=2$) transition for on-resonance excitation to the nonadiabatically perturbed C $^1\Pi_u^+$ ($\nu_i=3,J_i=1$) level ($\Delta_2=-9.56$ cm^{-1}) are exhibited in Figs. 4(a) and 4(b), with I_P^0 (I_S^0) $=1\times10^6$ W/cm^2 and 2

FIG. 5. Same as Fig. 4(b) except for the S-branch ($J_f = 2$) fundamental ($\nu_f = 1$) transition.
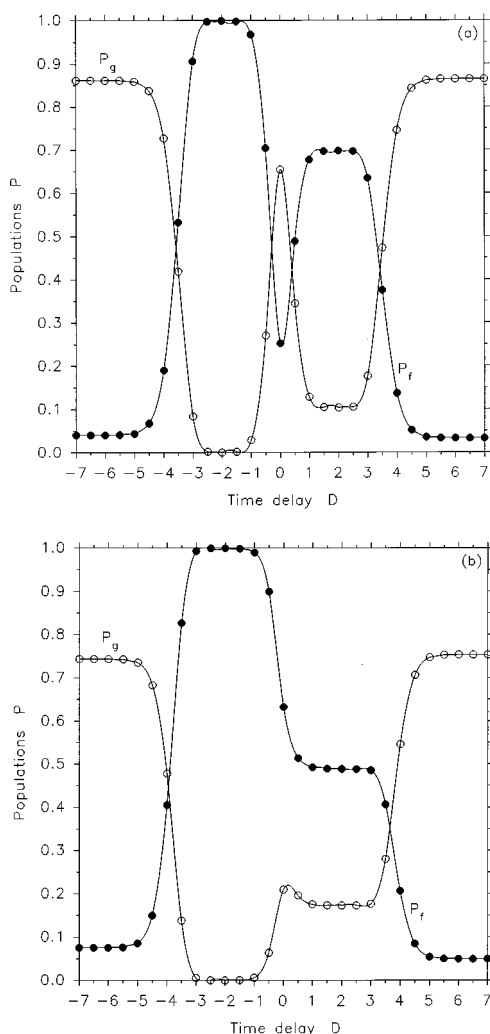

FIG. 4. Populations of the ground (P_g) and final (P_f) levels (after the pump and Stokes laser pulses are over) plotted against (reduced) time delay ($D = \Delta t / \tau_p$) between the pulses for the Q-branch ($J_f = 0$) first overtone ($\nu_f = 2$) transition from the $X(\nu_g = 0, J_g = 0)$ level for resonance with the intermediate perturbed $C(3,1)$ level for $\tau_p = 170$ ns and different values of I_P^0 (I_S^0) including the NA interaction between $B(14,1)$ and $C(3,1)$ levels. (a) I_P^0 (I_S^0) = 1×10^6 W/cm^2 and (b) I_P^0 (I_S^0) = 2×10^6 W/cm^2.

$\times 10^6$ W/cm^2, respectively. For I_P^0 (I_S^0) = 1×10^6 W/cm^2, the P_f profiles show strong asymmetry with double and broad peaked structure [Fig. 4(a)]. Transfer efficiency is 100% around $D = -2$ while the transfer is about 70% around $D = +2$. For I_P^0 (I_S^0) = 2×10^6 W/cm^2 [Fig. 4(b)], complete population transfer occurs with a broader peak around $D = -2$ but the transfer is reduced to about 50% with a shoulder around $D = +2$. It is important to mention here that for Q-branch fundamental ($\nu_f = 1$) transition the population transfer is negligible for resonance with the perturbed $C(3,1)$ level for all values of I_P^0 (I_S^0) considered. This is an interesting feature. This fact arises basically from the different transition matrix elements between the intermediate $C(3,1)$ and final levels in the two cases corresponding to $\nu_f = 1$ and $\nu_f = 2$ as seen in Table I. The population profiles corresponding to the on-resonance excitation to the perturbed $B(14,1)$ level ($\Delta_1 = 1.79$ cm^{-1}) for Q-branch first overtone ($\nu_f = 2$) transi-
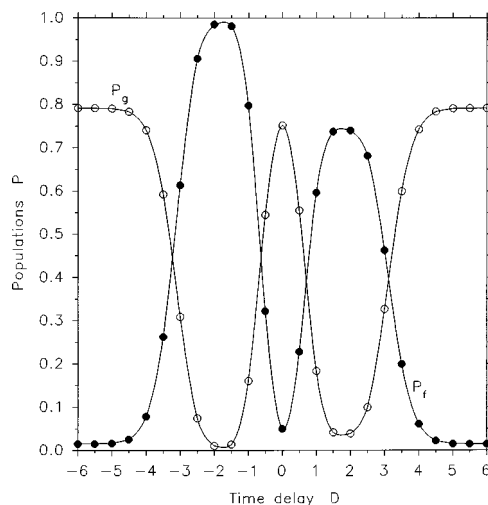
tion are not presented as they are almost similar to those for fundamental ($\nu_f = 1$) transition. The corresponding off-resonance profiles for $J_f = 0$ and $\nu_f = 2$ ($\Delta_1 = -8.61$ cm^{-1}) are also not presented because of very insignificant population transfer.

Figure 5 shows the population profiles for S-branch ($J_f = 2$) fundamental ($\nu_f = 1$) transition for on-resonance excitation with the perturbed $C(3,1)$ level ($\Delta_2 = -9.56$ cm^{-1}) for I_P^0 (I_S^0) = 2×10^6 W/cm^2. Almost total population transfer ($\sim 99\%$) occurs to the final level at $D \simeq -2$ and about 75% transfer takes place at $D \simeq +2$. It should be noted here that the population profiles for the S-branch fundamental transition for on-resonance excitation to the perturbed $B(14,1)$ level ($\Delta_1 = 1.79$ cm^{-1}) are almost the same to the corresponding Q-branch fundamental transition and hence are not shown.

In Fig. 6, the population profiles are drawn assuming the ABO approximation (i.e., making $V_{12} = 0$) for on-resonance and off-resonance excitations at I_P^0 (I_S^0) = 2×10^6 W/cm^2 for the Q-branch ($J_f = 0$) fundamental ($\nu_f = 1$) transition.

Figure 6(a) shows the population profiles when the pump-laser frequency is tuned to resonance with the unperturbed ABO $B(14,1)$ level ($\Delta_1 = 0$). The profiles for both the final and ground levels are remarkably changed from those obtained in Fig. 2(c) where the NA interaction between the two intermediate levels is taken into account. Thus it is seen that the electronic-rotational coupling between levels $B(14,1)$ and $C(3,1)$ due to intramolecular configuration interaction plays a very significant role in determining the population transfer efficiency. When the Stokes pulse precedes the pump pulse by more than $6 \tau_p$ ($D = -6$), the final level population P_f evolves because of spontaneous emission from the intermediate levels to the final level. This process accounts for the constant small value at $D < -6$. The population P_g of the ground level is almost zero because the pump intensity depletes it. Optimal transfer ($\sim 98\%$) is obtained when the Stokes pulse precedes the pump pulse by about $2 \tau_p$ ($D \simeq -2$) and partially overlaps the pump pulse. For $D = 0$ the final level population is significantly reduced relative to the optimal and appreciable population ($\sim 20\%$) remains in the ground level. For $D > 0$ there is no significant population transfer to the final level.
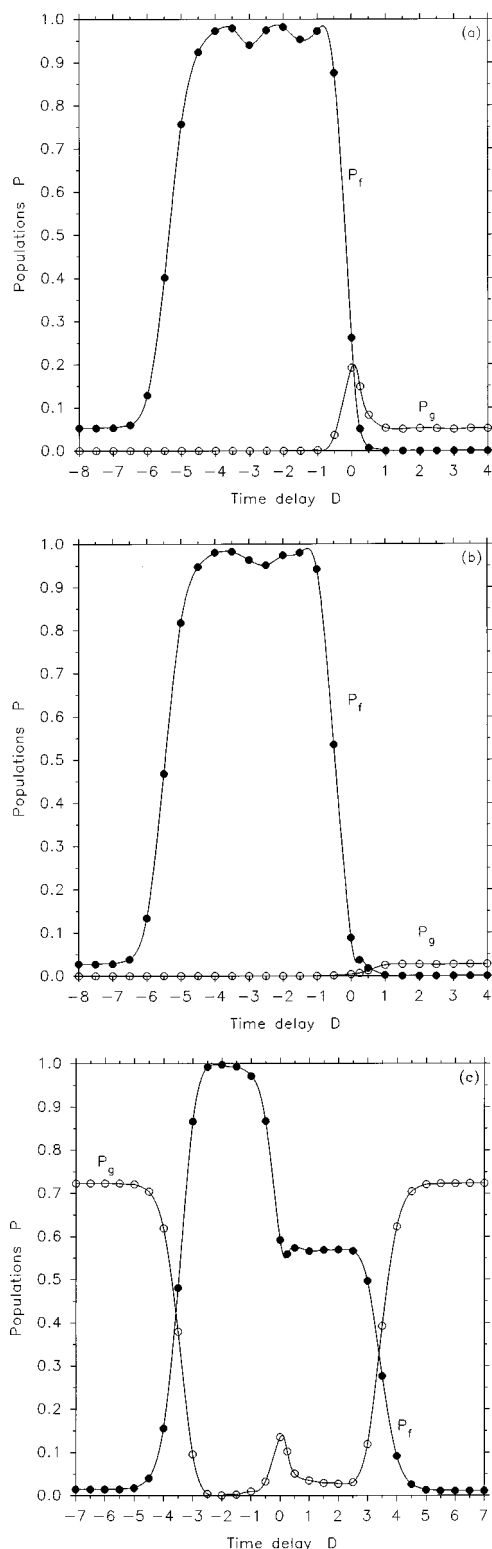
FIG. 6. (a) Same as Fig. 2(c) except for the ABO approximation ($V_{12}=0$) and resonance with the unperturbed (ABO) $B(14,1)$ level, (b) same as Fig. 6(a) except for resonance with the unperturbed (ABO) $C(3,1)$ level, and (c) same as Fig. 6(a) except for the frequency of the pump laser detuned by 1.79 cm^{-1} with respect to the unperturbed $B(14,1)$ level.

Figure 6(b) exhibits the population profiles for resonance with the unperturbed ABO $C(3,1)$ level ($\Delta_2=0$). The maximum transfer ($\sim 98\%$) occurs at $D \simeq -1.5$. Comparison with

the results considering NA interaction reveals the critical effect of the NA interaction on population distribution in the final level. As we have mentioned earlier, the profiles for on-resonance excitation to the $C(3,1)$ level with NA interaction are not presented because of the insignificant transfer efficiency. No appreciable population transfer takes place for $D > 0$ in this case also.

Figure 6(c) displays the population profiles when the pump-laser frequency is detuned by $\Delta_1 = 1.79$ cm^{-1} with respect to the unperturbed ABO $B(14,1)$ level. Complete transfer is achieved around $D = -2$ with a wide peak and about 58% population resides in the final level around $D = +2$ with a shoulder.

The population profiles using the ABO approximation (i.e., with $V_{12}=0$) for the four-level H$_2$ system as depicted in Fig. 6 are similar to the profiles presented by Band and Julienne [1(a)] for the three-level Na$_2$ system. The distortions (ups and downs) around $D = -2$ in the profiles in Figs. 6(a) and 6(b) are due to the presence of two intermediate levels (assuming no NA interaction between them) for our H$_2$ system.

V. CONCLUSION

We have investigated the population transfer from the ground to higher rovibrational final levels via two intermediate levels (belonging to electronically excited states) coupled with each other by nonadiabatic interaction in H$_2$ molecule in the presence of time-dependent overlapping pump and Stokes laser pulses. We have shown in detail the dependence of the final populations of the ground and final levels on the time delay between the two pulses for the cases of on-resonance as well as off-resonance excitations and for a wide range of peak intensities I_P^0 (I_S^0) of the pump (Stokes) fields. Two-photon Raman transitions to different final levels have been considered. For each case of excitation, the transfer efficiency is found to be very sensitive to the variation of peak intensities of the fields. Our calculations for the four-level H$_2$ system reveal that almost complete population is transferred in counterintuitive pulse order for both on-resonance and off-resonance excitations with intermediate and high values of I_P^0 (I_S^0). In intuitive pulse sequence also a large transfer is achieved for on-resonance excitation at intermediate values of I_P^0 (I_S^0), which is in contrary to the results of three-level system (viz., Na$_2$). For off-resonance excitation also a large transfer occurs at intermediate and high values of I_P^0 (I_S^0) in case of intuitive pulse order. To examine the effects of electronic-rotational coupling between the intermediate levels on the transfer efficiency the same calculations are done in some particular cases using ABO approximation. The results with ABO approximation differ remarkably from those obtained including NA interaction. It is to be mentioned that population profiles with ABO approximation are similar to the profiles presented by Band and Julienne [1(a)] for the three-level Na$_2$ system. In our study we have included the contributions of all possible rotational and magnetic sublevels into the calculations of state to state spontaneous radiative decay rates as the spontaneous emission couples different magnetic sublevels of the molecules in a different manner. It may be mentioned here that the cross coupling of different M levels by spontaneous emission will

not occur in our calculation since we have taken $J_g = 0$ (hence, $M_g = 0$) and linear parallel polarizations of the two laser fields.

About a decade ago, XUV (extreme ultraviolet) lasers ($<$100-nm wavelength) of 50-ns pulse duration and 3×10^{12}-W/cm^2 peak intensity were generated [15]. Earlier, vuv (vacuum ultraviolet) tunable lasers of 55-ns pulse duration and 1.6×10^9-W/cm^2 peak intensity were generated with 193-nm wavelength [16]. We hope that with the advancement of current technology, experiments with the values of laser parameters similar to those used by us will soon be feasible.

---

[1] (a) Y. B. Band and P. S. Julienne, J. Chem. Phys. **94**, 5291 (1991); (b) **95**, 5681 (1991); **97**, 9107 (1992); (c) Y. B. Band, Phys. Rev. A **45**, 6643 (1992).

[2] N. V. Vitanov and S. Stenholm, Opt. Commun. **127**, 215 (1996); **135**, 394 (1997); Phys. Rev. A **55**, 648 (1997); **55**, 2982 (1997); **56**, 741 (1997); **56**, 1463 (1997).

[3] (a) U. Gaubatz, P. Rudecki, M. Becker, S. Schiemann, M. Külz, and K. Bergmann, Chem. Phys. Lett. **149**, 463 (1988); J. R. Kuklinski, U. Gaubatz, F. T. Hioe, and K. Bergmann, Phys. Rev. A **40**, 6741 (1989); G-Z. He, A. Kuhn, S. Schiemann, and K. Bergmann, J. Opt. Soc. Am. B **71**, 1960 (1990); (b) U. Gaubatz, P. Rudecki, S. Schiemann, and K. Bergmann, J. Chem. Phys. **92**, 5363 (1990).

[4] R. G. Unanyan, N. V. Vitanov, and S. Stenholm, Phys. Rev. A **57**, 462 (1998).

[5] P. S. Julienne, J. Mol. Spectrosc. **48**, 508 (1973); A. L. Ford, *ibid.* **53**, 364 (1974); J. R. Burciaga and A. L. Ford, *ibid.* **149**, 1 (1991).

[6] S. Banerjee, S. S. Bhattacharyya, and S. Saha, J. Raman Spectrosc. **24**, 317 (1993); S. Ghosh, S. S. Bhattacharyya, and S. Saha, J. Chem. Phys. **107**, 5332 (1997).

[7] S. Ghosh, S. S. Mitra, S. S. Bhattacharyya, and S. Saha, J. Phys. B **29**, 3109 (1996).

[8] L. Wolniewicz and K. Dressler, J. Chem. Phys. **88**, 3861 (1988); **85**, 2821 (1986).

[9] W. Kolos, K. Szalewicz, and H. Z. Monkhorst, J. Chem. Phys. **84**, 3278 (1986); W. Kolos and L. Wolniewicz, *ibid.* **41**, 3663 (1964); A. L. Ford, A. M. Greenawalt, and J. C. Browne, *ibid.* **67**, 983 (1977).

[10] L. Wolniewicz, J. Chem. Phys. **51**, 5002 (1969).

[11] N. E. Greville, in *Mathematical Methods for Digital Computers*, edited by A. Ralston and H. S. Wilf (Wiley, New York, 1967), Vol. 2, p. 156.

[12] J. W. Cooley, Math. Comput. **15**, 363 (1961).

[13] P. Senn, P. Quadrelli, and K. Dressler, J. Chem. Phys. **89**, 7401 (1988).

[14] A. C. Allison and A. Dalgarno, At. Data **1**, 289 (1970); T. L. Stephens and A. Dalgarno, J. Quant. Spectrosc. Radiat. Transf. **12**, 569 (1972).

[15] H. Daido, E. Miura, Y. Kitagawa, Y. Kato, K. Nishihara, S. Nakai, and C. Yamanaka, in *Short-Wavelength Lasers and Their Applications*, edited by C. Yamanaka (Springer, Berlin, 1988), p. 105.

[16] S. C. Wallace, in *Photophysics and Photochemistry in the Vacuum Ultraviolet*, edited by S. P. McGlynn, G. L. Findley, and R. H. Huebner (Reidel, Holland, 1985), p. 105.